A potential distribution approach to fused heterochain molecules. I. Mixtures of hard dumbbells and spheres

1 AUTHOR:

Lloyd L. Lee

California State Polytechnic University, Pom…

139 PUBLICATIONS   **2,536** CITATIONS

A potential distribution approach to fused heterochain molecules. I. Mixtures of hard dumbbells and spheres

Lloyd L. Lee

School of Chemical Engineering and Materials Science, University of Oklahoma, Norman, Oklahoma 73019

We apply the potential distribution theorems for the cavity distribution functions to the development of thermodynamic formulas for fused-sphere chain molecules. Alternative forms of the potential distribution theorems are derived: in terms of the cavity functions, and in terms of the singlet direct correlation functions. We point out the connections to integral equation theories. To determine the behavior of fused dispheres, we examine the successful Wertheim thermodynamic perturbation theory (TPT) at different bond lengths l in light of the cavity functions. For ternary mixtures of spheres S and B, and fused dispheres (SB), we discover a *confluence point* where all cavity functions at different mixture compositions converge. This takes place at the tangent disphere limit $l=d$ (l being the bond length, and d, the hard sphere diameter). This point is also in common with the excess Helmholtz free energy from the TPT theory for tangent dumbbells. The cavity functions are obtained from the accurate equation of state of Boublík. To verify the chemical potentials calculated, we compare with new Monte Carlo simulations for mixtures of hard spheres and dumbbells. TPT does not hold for $l<d$. In order to have a quantitative expression for fused disphere properties, we propose an interpolation formula that performs well for both symmetric dispheres and asymmetric dispheres. This formula, though empirical, performs better than similar interpolative schemes proposed by Phan–Kierlik–Rosinberg. We have also derived purely thermodynamic formulas based on the TPT theory. These formulas can be exploited if one uses many of the existing thermodynamic properties correlations for mixtures. © *1995 American Institute of Physics.*

I. INTRODUCTION

The molecular theories of chain molecules composed of segmental spheres have developed to a high degree of sophistication and accuracy through works on the thermodynamic perturbation theory (TPT) by Wertheim,[1] the density functional theory of Kierlik and Rosinberg,[2] the generalized Flory dimer (GFD) theory by Hall *et al.*,[3] the integral equations with connectivity conditions by Chiew,[4] and the polymer RISM (PRISM) theory by Curro and Schweizer.[5] These theories have been applied not only to linear chains, but also to ringed, and branched chain molecules. Comparison with simulation data showed that they have achieved remarkable accuracy compared with earlier attempts. Chapman *et al.*[6] and Jackson *et al.*[7] have developed the Wertheim TPT first order theory (TPT1) to the extent of actual calculation for hydrogen-bonding liquid mixtures. Phase equilibria of associating fluid mixtures were successfully modeled.[8] For most cases, chain molecules are modeled as homonuclear tangent polyspheres without any attractive, polar, or charge forces. Recently, "tangent" Lennard-Jones polyspheres have been investigated.[9] Intensive activities on associated Lennard-Jones spheres have taken place.[10] Attempts have been made to generalize to liquid crystals and polymeric molecules.[11]

In this series, we initiate work on the polyspheric chains whose constituent spheres are *fused* (not tangent) and are of *different sizes* (heteronuclear). We call these the fused heterochain molecules (or fused heteropolyspheres). The implications to industrially important chemicals (hydrocarbons, polymers, etc.) are evident. Some earlier efforts[12] have been made within the framework of TPT1. For example, in 1990 Walsh and Gubbins[12] have used an effective segment number ν_e to model different degrees of fusion for heteropolyspheres

up to six segments by requiring the second virial coefficient B_2 of the *tangent* ν_e spheres obtained from TPT1 to be equal to the B_2 of the actual fused heteropolyspheres [say, from the scaled particle theory[13] (SPT)]. Accurate reproduction of simulation results for the compressibility was attained for many types of fused chains. For example, the fused tetramers (modeling united-atom normal butane molecules) were not represented by $\nu=4$ segments, but rather by $\nu_e=1.62$ fractional segments. In a similar vein, Amos and Jackson[12] required that the geometric shape ratio $\alpha \equiv \bar{r}s/3b$ be the same for the *tangent* polyspheres as for the fused polyspheres. ($\bar{r}$ is the mean radius of curvature of an equivalent convex body; s, the actual *exposed* surface area of one fused chain, and b, its volume.) Again, good representation of simulation data on compressibility was obtained. In Walsh–Gubbins, the modified TPT1 equation was the same as the original *homonuclear* tangent polysphere TPT1, except the segment number was altered from an actual ν to an effective ν_e, irrespective whether the original fused polyspheres were heteronuclear or homonuclear. In Amos–Jackson, the TPT1 equation used allowed for heteronuclear tangent polyspheres. However, the diameter ratio d_2/d_1 was treated as an "adjustable" parameter in order to match the geometric shape factor α of an actual fused heteropolysphere. For example, for the case of homonuclear fused dispheres with 80% fusion (bond length l is 20% of the hard sphere diameter d: $l=0.2d$), the actual $\alpha=1.0185$. Thus d_2/d_1 was fitted to 0.1 (namely, for the TPT equation, a heteronuclear dimer of two tangent spheres was used: where the big sphere had diameter d_1 and the small sphere had diameter $0.1d_1$). In both approaches, the pictures (fractional segments and/or uneven spheres) of the equivalent tangent chains for use in TPT1 could be quite different from the actual fused chains. Could this be rem-

edied on a more fundamental level? We shall attempt a different perspective.

The approach we shall adopt here is the potential distributions in the integral equation theory of liquids, in particular the cavity distribution functions (or cdf, the cavity functions). The cavity distribution function $y(r)$ is defined in terms of the pair correlation function $g(r)$ (e.g., for spherically symmetric molecules) via

$$y(r) \equiv g(r) e^{\beta u(r)}, \tag{1.1}$$

where $u(r)$ is the pair potential energy, $\beta = 1/kT$, the reciprocal temperature, and k, the Boltzmann constant. A number of interesting theorems exist for the cdf, such as the zero-separation theorems (ZST)[14] the potential distribution theorems (PDT),[15] and the integral equation theories on closures (PY, HNC,[16] and VM,[17] etc.). What is of direct interest are the potential distribution theorems which have already been extensively used in the computer simulations[18] for chemical potentials of many kinds of molecules (Lennard-Jones, polar,[19] charged, polymeric,[20] etc.). Recently, it has been shown that the cavity functions are related to the chemical potentials of polyatomic molecules through these potential distributions.[21] Thus the chain molecules will constitute a natural subject of investigation under the potential distribution formalism.[22] Some pioneering work has been done, notably by Zhou and Stell[23] in a series of papers since 1989. In their approach, contacts were made with the successful Wertheim TPT by elucidating the theoretical basis of TPT through the approximations made to higher nth-order cavity functions $y^{(n)}$, a quite different way of analysis from the two-density cluster expansion approach of Wertheim.[1]

In this work, we intend to proceed further with the cavity function analysis by providing three potential distribution theorems, some are newly derived, (i) to show where TPT1 works and where improvements are needed, and to propose effective methods that accurately treat fused spheres. (ii) To provide a general theoretical framework for treating fused heteropolyspheres interacting with general potentials (Lennard-Jones, charged, etc.). (iii) To derive thermodynamic formulas that express the remarkable Wertheim intuition in a different perspective. (iv) To test the new methods, as an illustration, on simple fused dispheres. In subsequent works, we shall extend to more realistic potential models and longer chains. This work differs from previous studies in not only providing a more general theoretical background (the PDT's, the new thermodynamic formulas, connections to singlet dcf), but also giving quantitatively accurate free energy and pressure formulas for fused dispheres at any bond length, $0 \leq L \leq 1$ (where L is the reduced bond length, l/d). These serve as basis for tackling higher chain lengths.

In Sec. II, we shall state and derive, when needed, the potential distribution theorems for monomeric, dimeric, and trimeric molecules. Generalizations to higher oligomers are obvious. We relate further these formulas to the nonuniform singlet direct correlation function (dcf) $C_a^{(1)}(\mathbf{r}_N; w)$ under the influence of an external potential, w. The singlet dcf plays a pivotal role[24] in integral equation theories as well as density functional theories. We shall bring these techniques to bear

on the question at hand. In Sec. III, we apply the first two PDT's to the test cases of symmetric and asymmetric fused dumbbells. Their binary and ternary mixtures with monospheres are investigated by employing highly accurate equations of state from Tildesley and Streett,[25] and Boublík.[26] We examine the performance of Wertheim's TPT1 for dispheres at different degrees of fusion. We propose a new interpolation formula that is based on a suggestion of Phan–Kierlik–Rosinberg (PKR).[27] We scale all calculations by the same packing fraction η as proposed by PKR. This new empirical formula accurately represents the fused sphere Helmholtz free energy from $L=0$ to 1. We discover that the probability of inserting a sphere into a pure dimer fluid (i.e., the chemical potential) depends on the "available space" therein as proposed by Speedy and Reiss,[28] this being easier than insertion into pure spheres. To ascertain this behavior, we verify with new Monte Carlo simulations. For all the cavity functions at the same packing fraction but with different compositions of the mixture, a converging point is discovered at bond lengths equal to the distance where tangent disphere is formed (e.g., at $L=1$ for symmetric dispheres). That there is such a convergence point is a remarkable behavior. This point also coincides with the TPT1 expression of the Helmholtz free energies for tangent dispheres as expected. Away from this point ($L<1$), TPT1 does not work well, as noted in the Zhou–Stell studies. In Sec. IV, we discuss the relation of the present work to Zhou and Stell's and to TPT1. In addition, we derive thermodynamic formulas that can equally express many features of TPT1 solely in terms of macrothermodynamically accessible variables. This is done through the Kirkwood–Buff[29] fluctuation integrals. Section V presents the conclusions.

II. THE POTENTIAL DISTRIBUTION THEOREMS

In the following we shall present three potential distribution theorems (PDT) and their alternative forms in terms of the singlet direct correlation function. Some are a review, and some are new. We consider, without loss of generality, a mixture of two species a and b, with mole fractions x_a and x_b in a given volume V and under given pressure P and temperature T. The first member of the PDT was derived by Widom[30] (prime indicates configurational properties).

The first potential distribution theorem

$$\beta \mu_a' = -\ln\langle \exp[-\beta \Psi_a(; \mathbf{r}_N)]\rangle_{N-1}. \tag{2.1}$$

Namely, in the language of computer simulation, the configurational (excess) chemical potential $\beta \mu_a'$ of a in a mixture at the state (x_a, x_b, T, P, V) can be obtained from the $(N-1)$ particle (excluding the test particle) ensemble average of the excess potential Ψ due to a test particle of type a located at $\mathbf{r}_N$. $\Psi(; \mathbf{r}_N) \equiv \sum_{j=1}^{N-1} u_{ja}(\mathbf{r}_j, \mathbf{r}_N)$. In computer simulations, many "fictitious" particles are injected at random into the $(N-1)$ particle mixture to sample the contribution from $\langle \exp(-\beta \Psi_a)\rangle_{N-1}$.

The second potential distribution theorem[21] is concerned with the contributions from two test particles of species a and b located at $\mathbf{r}_N$ and $\mathbf{r}_{N-1}$, respectively, *the second potential distribution theorem*

$$\ln y_{ab}(\mathbf{r}_N,\mathbf{r}_{N-1}) = \beta\mu'_a + \beta\mu'_b + \ln\langle\exp[-\beta\Psi_a(;\mathbf{r}_N)$$
$$-\beta\Psi_b(;\mathbf{r}_{N-1})]\rangle_{N-2}. \quad (2.2)$$

Thus the potential distribution in an $(N-2)$-body ensemble of a pair of test particles gives the cavity distribution function y_{ab}. These theorems are completely general as far as the interaction pair potentials are concerned. They could be hard core, Lennard-Jones, or polar, polyatomic ones. As the two test particles approach each other to form a bond of length $l=|\mathbf{r}_N-\mathbf{r}_{N-1}|$, or in reduced units $L_{ab}=l/d$, the potential distribution term can be viewed as the configurational chemical potential of the dimer (ab) [i.e., the probability of inserting a dimer (ab) of bond length L_{ab} into a given mixture of species a and b]. Thus Eq. (2.2) can be written as

$$\ln y_{ab}(L_{ab}) = \beta\mu'_a + \beta\mu'_b - \beta\mu'_{(ab)}(L_{ab}), \quad (2.3)$$

where, we have applied the first PDT,

$$\beta\mu'_{(ab)} = -\ln\langle\exp[-\beta\Psi_a(;\mathbf{r}_N)-\beta\Psi_b(;\mathbf{r}_{N-1})]\rangle_{N-2}. \quad (2.4)$$

This dimer (ab) is by the present construction at infinite dilution. However, if to begin with, we have a ternary mixture of a, b, and (ab) species with mole fractions $(x_a, x_b, x_{(ab)})$, then this insertion is at any finite mole fractions of the dimer. Next we inquire as to what happens when three test particles are being potential-distributed. By the same token, we have *the third potential distribution theorem*

$$\ln y^{(3)}_{abc}(\mathbf{r}_N,\mathbf{r}_{N-1},\mathbf{r}_{N-2})$$
$$= \beta\mu'_a + \beta\mu'_b + \beta\mu'_c - \beta\mu'_{(abc)} = \beta\mu'_a + \beta\mu'_b + \beta\mu'_c$$
$$+ \ln\langle\exp(-\beta\Psi_a(;\mathbf{r}_N)-\beta\Psi_b(;\mathbf{r}_{N-1})$$
$$-\beta\Psi_c(;\mathbf{r}_{N-2}))\rangle_{N-3}, \quad (2.5)$$

where $\beta\mu'_{(abc)}$ is the configurational chemical potential (at infinite dilution) of the trimer (abc) in an $(N-3)$-body ensemble. $y^{(3)}$ is the triplet cavity function. We need the first two PDT's for dimeric fluids. We shall need the third PDT for trimeric fluids.

As pointed out in an earlier study,[31] the potential distributions are closely associated with the singlet direct correlation function $C^{(1)}$ under an external potential field $w(.)$

$$C^{(1)}_a(\mathbf{r}_N;w) \equiv \ln(\rho^{(1)}_a(\mathbf{r}_N;w)\Lambda^3_a) + \beta w_a(\mathbf{r}_N) - \beta\mu_a. \quad (2.6)$$

When the external potential w is generated by a test particle of species b at position $\mathbf{r}_{N-1}$,

$$w_a(\mathbf{r}) \equiv u_{ab}(\mathbf{r},\mathbf{r}_{N-1}) \quad (2.7)$$

the singlet dcf gives the *alternative second potential distribution theorem*

$$-\beta\mu'_{(ab)} = \ln\langle\exp(-\beta\Psi_a(;\mathbf{r}_N)-\beta\Psi_b(;\mathbf{r}_{N-1}))\rangle_{N-2}$$
$$= C^{(1)}_a(\mathbf{r}_N;w=u_{ab}) - \beta\mu'_b. \quad (2.8)$$

When $w=0$ in a uniform system, we recover the *alternative first potential distribution theorem*

$$-\beta\mu'_a = \ln\langle\exp(-\beta\Psi_a(;\mathbf{r}_N))\rangle_{N-1} = C^{(1)}_a(\mathbf{r}_N;w=0). \quad (2.9)$$

We remark here that contact can now be made with a recent scaled particle theory (SPT) approach of Labik–Malijevsky–Smith[32] (LMS) on chain molecules that was derived from geometric arguments and the YBG (Yvon–Born–Green[33]) hierarchy. In the LMS approach, the chemical potential $\mu^{(n)}$ (or *work needed for insertion*) of an n sphere in a bath of monospheres is the sum of the chemical potential $\mu^{(n-1)}$ of the $(n-1)$-sphere and the work $w^{(n)}$ required to "grow" a new sphere from one end of the $(n-1)$-spherical chain and eventually reaching a bond length l away from the end (we shall discuss only the configurational contributions below)

$$\beta\mu'^{(n)} = \beta\mu'^{(n-1)} + \beta w^{(n)}(l),$$

or

$$\beta\mu'^{(2)} = \beta\mu'^{(1)} + \beta w^{(2)}(l) \quad \text{for } n=2. \quad (2.10)$$

Comparison with Eq. (2.8) gives

$$w^{(2)}_a(l) = -C^{(1)}_a(\mathbf{r}_N;w=u_{ab})]|_{\mathbf{r}_N-\mathbf{r}_{N-1}|=l}. \quad (2.11)$$

Namely, the work required to grow a new sphere a to position $\mathbf{r}_N$ from the existing sphere b at $\mathbf{r}_{N-1}$ is given by the negative singlet dcf $C^{(1)}_a(\mathbf{r}_N; w=u_{ab})$. Therefore, we have acquired a SPT-frame interpretation of the singlet dcf: *as the work term for creating new segments (cavities) from existing polyspheres.* Next, we shall derive the alternative form of the third PDT in terms of the nonuniform singlet dcf. When the external field is generated by a pair of test particles b and c

$$w_a(.) = u_{ab}(.,\mathbf{r}_{N-1}) + u_{ac}(.,\mathbf{r}_{N-2}),$$

$$C^{(1)}_a(\mathbf{r}_N;w=u_{ab}+u_{ac}) = \ln\rho^{(1)}_a(\mathbf{r}_N;w=u_{ab}+u_{ac})\Lambda^3_a + \beta u_{ab}(\mathbf{r}_N,\mathbf{r}_{N-1}) + \beta u_{ac}(\mathbf{r}_N,\mathbf{r}_{N-2}) - \beta\mu_a$$

$$= \ln\rho_a\Lambda^3_a - \beta\mu_a + \ln\left(\frac{g^{(3)}_{abc}(\mathbf{r}_N,\mathbf{r}_{N-1},\mathbf{r}_{N-2})}{g^{(2)}_{bc}(\mathbf{r}_{N-1},\mathbf{r}_{N-2})}\right) + \beta u_{ab}(\mathbf{r}_N,\mathbf{r}_{N-1}) + \beta u_{ac}(\mathbf{r}_N,\mathbf{r}_{N-2})$$

$$= \ln y^{(3)}_{abc}(\mathbf{r}_N,\mathbf{r}_{N-1},\mathbf{r}_{N-2}) - \ln y^{(2)}_{bc}(\mathbf{r}_{N-1},\mathbf{r}_{N-2}) - \beta\mu'_a. \quad (2.12)$$

Thus the *alternative third potential distribution theorem*

$$-\beta\mu'_{(abc)} = \ln\langle\exp(-\beta\Psi_a(;\mathbf{r}_N)-\beta\Psi_b(;\mathbf{r}_{N-1})-\beta\Psi_c(;\mathbf{r}_{N-2}))\rangle_{N-3}$$

$$= C^{(1)}_a(\mathbf{r}_N;w=u_{ab}+u_{ac}) + C^{(1)}_b(\mathbf{r}_{N-1};w=u_{bc}) + C^{(1)}_c(\mathbf{r}_{N-2};w=0). \quad (2.13)$$

The indices a, b, and c are equivalent and can be permuted with the same result. Noting that from Eq. (2.10), $\mu'^{(3)} = \mu'^{(2)} + w^{(3)}$, we have again

$$\beta w_a^{(3)} = -C_a^{(1)}(\mathbf{r}_N; w = u_{ab} + u_{ac}). \tag{2.14}$$

Namely, given spheres b and c at $\mathbf{r}_{N-1}$ and $\mathbf{r}_{N-2}$, respectively, the work required to grow a new sphere a to the position $\mathbf{r}_N$ is given by the negative $C_a^{(1)}(\mathbf{r}_N; w = u_{ab} + u_{ac})$. In retrospect, Eq. (2.9) said that in the absence of a fixed test particle $(w = 0)$, the work $w_a^{(1)}$ required for producing a sphere (a cavity) of a in the fluid of monospheres was the chemical potential $\beta\mu_a'$ (a strictly SPT concept) and it was the negative of $C_a^{(1)}(\mathbf{r}_N; w = 0)$.

Here, we have derived a new expression for the trimer chemical potential in terms of the singlet dcf's. And the non-uniform singlet dcf is the negative of the *excess* work needed to create a cavity or to grow a new sphere of type a from the existing spheres b and c. The advantage of expressing the potential distributions in terms of the nonuniform singlet dcf is the connection to the entire paraphernalia of integral equation theorems. For example, the expansion of the singlet dcf gives the closure relation

$$C_a^{(1)}(\mathbf{r}_N; w) - C_a^{(1)}(\mathbf{r}_N; w = 0)$$
$$= \ln y_{ab}(\mathbf{r}_N, \mathbf{t}) = h_{ab}(\mathbf{r}_N, \mathbf{t}) - C_{ab}^{(2)}(\mathbf{r}_N, \mathbf{t}) + B_{ab}(\mathbf{r}_N, \mathbf{t}), \tag{2.15}$$

where $w(.) = u_{ab}(., \mathbf{t})$ and h, C, and B are the total, direct, and bridge correlations, respectively. $\mathbf{t}$ is the position vector of the test particle. Equation (2.15) incorporates the integral equation methods into the evaluation of $C_a^{(1)}(\mathbf{r}_N; w)$, and through the PDT's to chemical potentials of dimers, etc. For example, if we characterize the bridge function $B(r)$ for Lennard-Jones molecules,[34] we can go straight through the cavity function $\ln y(r)$ to fused Lennard-Jones dimeric fluids. Higher order dcf can be obtained from the hierarchy

$$\frac{\delta C_a^{(1)}(\mathbf{r}_N; w)}{\delta \rho_b^{(1)}(\mathbf{r}_{N-1})} = C_{ab}^{(2)}(\mathbf{r}_N, \mathbf{r}_{N-1}; w), \tag{2.16}$$

where δ/δ is the functional derivative operator. The pair direct correlation function $C_{ab}^{(2)}$ can be derived from the singlet dcf. So can the triplet dcf from the pair dcf. These equations are provided for future use.

III. APPLICATIONS TO FUSED HARD DUMBBELLS

We shall use the first and second PDT's for the characterization of the behavior of mixtures of hard single spheres (subscript S) and fused hard dispheres (subscript D) at arbitrary bond length L. Two types of dispheres are considered: fused symmetrical dispheres (diameters of constituent spheres $d_1 = d_2$), and fused heterodispheres (diameters of constituent spheres $d_1 \neq d_2$). The conditions are summarized below.

Mixtures of fused symmetric dispheres with monospheres:

(1) Packing fractions: $\eta = 0.1$, 0.3, and 0.47.
(2) Mole fractions: $x_D = 0.0$, 0.4, 0.7, and 1.0.

(3) Bond lengths: $L = l/d = 0.0$, 0.1, 0.2, 0.3, 0.4, 0.5, 0.6, 0.7, 0.8, 0.9, and 1.0.

Mixtures of fused heterodispheres with monospheres:

(1) Packing fractions: $\eta = 0.209$, 0.25, 0.30, 0.35, 0.367, 0.40, and 0.408.
(2) Mole fractions: $x_D = 0.0$, 0.2, 0.5, 0.7, and 1.0.
(3) Bond lengths: $L = l/d_S = 0.0$, 0.1, 0.2, 0.3, 0.4, 0.5, 0.6, 0.7, 0.8, 0.9, 1.0, 1.25, and 1.4925.
(4) Aspect ratio: $d_B/d_S = 1.19$, 1.2, 1.4925, 1.5, 1.8, and 2.0.

For pure dispheres, we have used two equations of state (EOS) to describe their thermodynamic properties: the very accurate Tildesley–Streett[25] (TS) equation and the equally valid Boublík[26] EOS (this has been checked and accuracy established here). The TS equation is accurate to within 0.4% on average (or maximum 1.1%) when compared to Monte Carlo data. However, the TS EOS does not describe mixtures of dispheres with hard spheres. We use the Boublík EOS for mixtures.

We can obtain the chemical potentials of the monospheres $\beta\mu_S'$ and $\beta\mu_B'$ (without possible ambiguity, assigning subscripts S to small spheres, and B to big spheres), as well as the dumbbell $\beta\mu_D'$ from the Boublík EOS in ternary mixtures via the prescription of Boublík 1986.[21] Then the unlike cavity function between S and B, $y_{SB}(L; \eta)$, can be obtained from the second potential distribution theorem as

$$\ln y_{SB}(L; \eta, x_S, x_B, x_D)$$
$$= \beta\mu_S'(\eta, x_S, x_B, x_D) + \beta\mu_B'(\eta, x_S, x_B, x_D)$$
$$\quad - \beta\mu_D'(L; \eta, x_S, x_B, x_D), \tag{3.1}$$

where we have explicitly shown the state conditions. Thus $\ln y_{SB}$ is evaluated at the mixture conditions with packing fraction η

$$\eta \equiv \frac{\pi}{6}(\rho_S d_S^3 + \rho_B d_B^3) + \rho_D V_D \tag{3.2}$$

and with the concentrations for equimolar small and big monospheres at $x_S = x_B$, and $x_D \geq 0$ for dumbbells. Thus the cavity function obtained corresponds to this given mixture (not set at some hypothetical reference state at infinite dilution $x_D = 0.0$ as in the Wertheim approach). Similarly, all the chemical potentials are evaluated at actual mixture composition (x_S, x_B, x_D) (not referred to the reference monospheres with $x_D = 0$). The disphere volume V_D is easily obtained from geometrical considerations.

A. Symmetric dispheres

For symmetric dispheres, $d_B = d_S$. The situation is simpler. We shall examine first the behavior of the cavity function at different mole fractions x_D and different bond lengths L. Figure 1 shows the cavity functions $\ln y_{SS}(L; \eta)$ of the monosphere–monosphere S–S pair as function of L at four concentrations $x_D = 0.0$ (infinitely dilute dispheres), 0.4, 0.7, and 1.0 (pure dispheres). Note that the packing fraction η has been fixed at 0.47. Since L changes from 0 (where disphere =monosphere) to 1 (the tangent disphere limit), the number densities of all species have to change to accommodate a
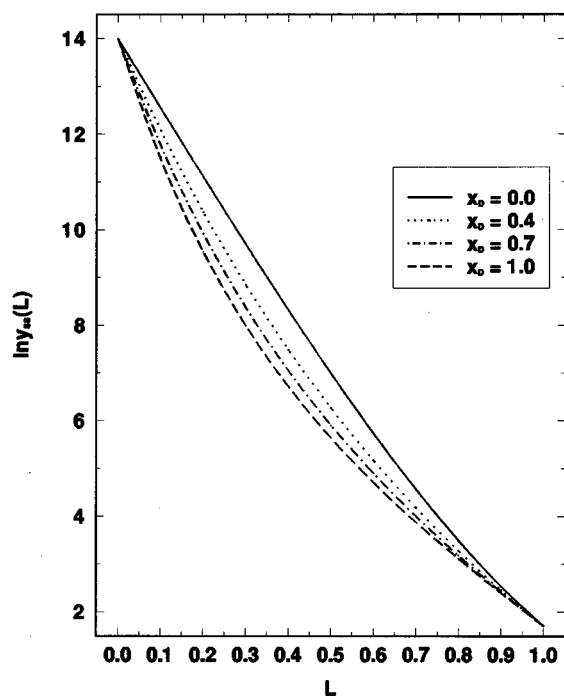
FIG. 1. Cavity functions $\ln y_{SS}$ of monosphere-monosphere pairs in mixtures of hard spheres+symmetric dispheres at different compositions. Packing fraction η is constant at 0.47. Four rows from top to bottom are at $x_D=0$, 0.4, 0.7. and 1. Note that the $\ln y_{SS}$ at all compositions merge to a single *confluence point* at $L=1$. This behavior is general for all the mixtures studied.
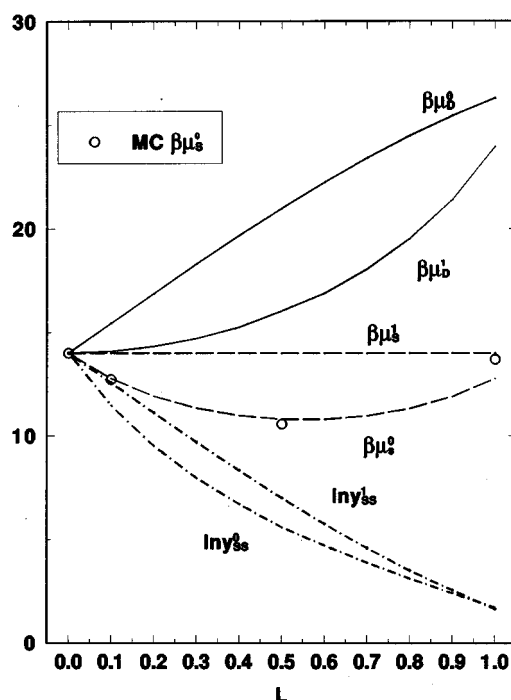
FIG. 2. Chemical potentials of mixtures of hard spheres+symmetric dispheres. Packing fraction $\eta=0.47$. Superscript 1 indicates pure state, while 0 indicates infinite dilution. The infinite dilution $\beta\mu_S^0<$pure $\beta\mu_S^1$, especially at $L\sim0.5$. Circles are MC simulation data to verify this behavior. Also $\beta\mu_D^1<\beta\mu_D^0$ at $L=1$. The test dimer (during test particle insertion) can tell the difference of the fluid types: pure tangent dimers, or pure monomers. It is easier to insert dimers into pure dimers than inserting into pure monomers at the same η.

constant η. We observe that even at constant η, the $S-S$ cavity functions are different at different x_D. *Thus there does not exist a "reference state" fluid (as in TPT1, the totally dissociated monosphere fluid) for which the cavity function y_{SS} can be used as a universal reference at any bond length $0<L<1$.* We note that our use of Eq. (3.1) is accurate to the extent that the underlying Boublík EOS is valid. The PDT2 itself is certainly and exact expression.

We found an interesting behavior in Fig. 1: within the present numerical accuracy, all $\ln y_{SS}(L;x)$ converge to a single point at bond length $L=1$ (at the right side of Fig. 1). At $L=0$, the left side of Fig. 1, all $\ln y_{SS}(L=0)$ also converge to a single value. The latter is not surprising, since as $L\rightarrow0$, all dispheres become monospheres, and are thus indistinguishable from single hard spheres at same η. We arrive at the pure hard sphere value, i.e., the zero separation theorem for hard spheres: $\ln y_{SS}(0)=\beta\mu_S'$ at η. However, that they all meet again at $L=1$ is a remarkable phenomenon. For ease of parlance, we shall refer to this point (at $L=1$) as the *confluence point*. At $L=1$, we have tangent dispheres (i.e., two spheres touching each other without fusion, with bond length $l=d$). One could argue (*the argument*) in plain terms that a tangent disphere upon insertion into a bath of molecules probably *does not know* the difference between a fluid of monospheres from a fluid of tangent dispheres (both at same η). In terms of chemical potentials, this would imply that the infinite dilution ($x_D=0.0$) chemical potential of a tangent disphere (in a bath of monospheres of the same η) should be equal to pure disphere chemical potential at

$x_D=1.0$ (this will be shown to be false). We want to examine this.

Figure 2 plots the infinite dilution chemical potential $\beta\mu_D'^0$ at $x_D=0$ together with the pure $\beta\mu_D'^1$ at $x_D=1$. (The superscripts "0" or "1" indicate the infinite dilution or pure state of the subscripted species, respectively.) We see that at $L=1$, these two values are quite different, $\beta\mu_D'^1(L=1)<\beta\mu_D'^0(L=1)$. This is not an isolated case, since at $\eta=0.3$, and 0.1, we also observe the same differences. This result suggests that it is easier to insert a disphere into pure dispheric fluid than to insert a disphere into a pure monospheric fluid $\beta\mu_D'^1<\beta\mu_D'^0$ even though the free volumes $(1-\eta)$ in both fluids are the same. This can be attributed to the fact that monospheres are more randomly dispersed in the free volume than dispheres, in the latter two spheres are linked, one is confined to the other. Thus the free volume in pure dispheres is such that it yields "higher opportunity" for inserting bodies than in pure monospheres. Speedy *et al.*[35] have introduced the concept of an "available space" V_0. It is the part of the free volume in which the center of a new sphere can be situated so that the incoming sphere will not overlap with the existing bodies. We can call this the *hospitality factor* (h.f.). Dispheres are more "hospitable" than monospheres at the same $1-\eta$. This effect is felt all way up to $L=1$ and does not disappear at that point. In formulas, the free volume is given by $V(1-\eta)$. Thus the h.f, is defined as

TABLE I. Constant N-P-T Monte Carlo simulation of infinitely dilute hard sphere chemical potentials in a symmetric fused disphere fluid of bond length L. MC: new Monte Carlo values. EOS: calculated from Boublík EOS.

η	N_{disphere}	$N_{\text{conf.}}$	L	MC $\beta\mu_S^{\prime 0}$	EOS $\beta\mu_S^{\prime 0}$
0.47	-	-	0	-	14.0
0.47	256	5E+06	0.1	12.7	12.774
0.47	256	5E+06	0.5	10.6	10.806
0.47	256	5E+06	1.0	13.7	12.8

$$\text{h.f.} \equiv \frac{V_0}{V(1-\eta)}. \qquad (3.3)$$

In the same Fig. 2, we have also plotted the single sphere chemical potentials $\beta\mu_S^{\prime 0}$ at $x_D=1$ and $\beta\mu_S^{\prime 1}$ at $x_D=0$. We see that the $\beta\mu_S^{\prime 1}$ is constant over L (i.e., pure monospheric μ is constant). The $\beta\mu_S^{\prime 0}$ at infinite dilution is for the most part smaller than the pure monospheric $\beta\mu_S^{\prime 1}$. Namely, it is easier to insert a single sphere into a pure disphere fluid than to do the same in pure monospheres at the same free volume faction $(1-\eta)$. Again, disphere have a higher hospitality factor. Speedy et al.[35] gave the chemical potential for hard core fluids

$$\beta\mu = \ln(\rho\Lambda^3) - \ln\left(\frac{V_0}{V}\right) = \ln(\rho\Lambda^3) - \ln(1-\eta) - \ln(\text{h.f.}). \qquad (3.4)$$

Thus the higher the h.f., the lower the chemical potential. [For point particle insertion, $V_0=$ free volume, and h.f.$=1$. Then $\ln(\text{h.f.})=0$.]

To check $\beta\mu_S^{\prime 0}$, we have carried out Monte Carlo simulations for the chemical potential of a single hard sphere in pure disphere fluids by the test particle insertion method. Three bond lengths $L=0.1$, 0.5, and 1.0 of disphere at $\eta=0.47$ were evaluated. About five million configurations were generated for each case. The results are presented in Table I.

The agreement with Boublík EOS results is excellent. Thus the Boublík results are considered dependable. At $L=1$, small difference remains in the MC chemical potential $\beta\mu_S^{\prime 0}$ from $\beta\mu_S^{\prime 1}$ of pure hard spheres, indicating that the monomer "knows" the difference between tangentially connected disphere from simply high density monospheres.

Equally, the fluid mixtures can tell the difference of inserting a disphere at different mole fractions. Thus the argument presented in the previous paragraphs is not valid. This makes the presence of a confluence point even more striking. It is the cancellation of all these subtle effects by the monomeric and dimeric chemical potentials through the second potential distribution theorem (3.1) that accounts for the confluence behavior.

To check if the TPT1 assumptions of Wertheim are also applicable here, (namely, if $\beta a_D' \approx 2\beta a_S' - \ln y_{SS}$), we have plotted the quantity, $\ln z(L;\eta)$, defined below in terms of configurational Helmholtz free energies: $\beta a_S' = \beta A_S'/N_S,...$
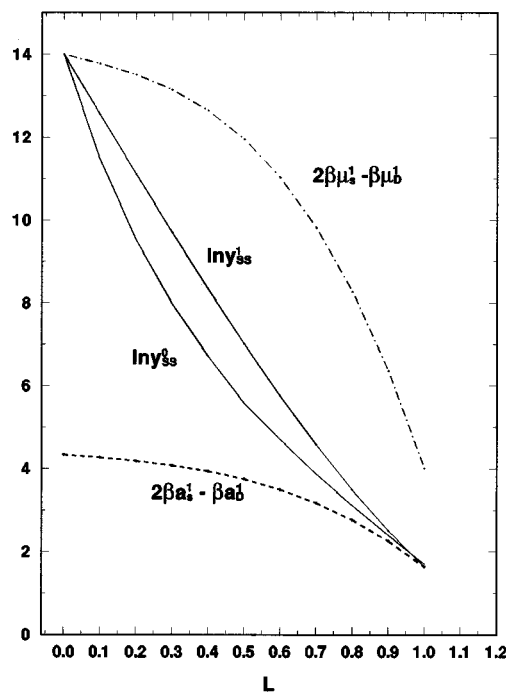

FIG. 3. Characterization of TPT1 for mixtures of hard spheres+symmetric disphere. Packing fraction $\eta=0.47$. Dashed line indicates TPT1: the Helmholtz free energy difference between pure disphere and pure monospheres. It should be equal to the cavity function $\ln y_{SS}^1$ according to TPT1. Differences are indication of the failure of TPT1. Only two cavity functions are shown: one for pure monomers $\ln y_{SS}^1$, the other at infinite dilution $\ln y_{SS}^0$. TPT1 is coincident with both $\ln y_{SS}$ at $L=1$, the confluence point (where TPT1 is valid). For $L\ll 1$, TPT1 value is different from all $\ln y$. Thus TPT1 is not valid for $L<1$ (see text). Note that at $L=1$, the chemical potentials do not converge to the common point!

$$x_D \ln z_{SS}(L;\eta,x_S=1,x_D=0)$$

$$\equiv (1+x_D)\beta a_S'(\eta,x_S=1,x_D=0)$$

$$- \beta a_D'(L;\eta,x_S\geq 0,x_D\geq 1). \qquad (3.5)$$

The compositions in the arguments of the first two terms are for the hypothetical reference fluid only. The x_i outside the arguments are actual mixture compositions. When $x_D=1$ (i.e., pure disphere), we simply have $\ln z(L) = 2\beta a_S^{\prime 1} - \beta a_D^{\prime 1}(L)$. If $\ln z(L)=\ln y_{SS}(L)$, then TPT1 is justified. Otherwise, TPT1 fails. Thus $\ln z$ is a kind of litmus test for TPT1. We note that in the TPT1 equation, the terms on either side of Eq. (3.5) do not refer to the same mixture. While terms involving single spheres are evaluated at pure monosphere concentration $x_S=1$ (i.e., pure reference fluid), the term for disphere is at the mixture mole fractions: a mixture of disphere and monospheres ($x_D\geq 0$ and $x_S\geq 0$). So this is a mixed-type equation, in contrast to PDT2 Eq. (3.1), where all terms refer to the same mixture at the same conditions. No reference fluid was used.

This $\ln z(L)$ at different L is plotted in Fig. 3 together with the cavity functions obtained earlier. We detect large differences between $\ln z(L)$ and $\ln y(L)$ in general. However, at $L=1$, all three curves $\ln z(L)$, $\ln y_{SS}^0(L)$, and $\ln y_{SS}^1(L)$ converge to the same confluence point. This indi-
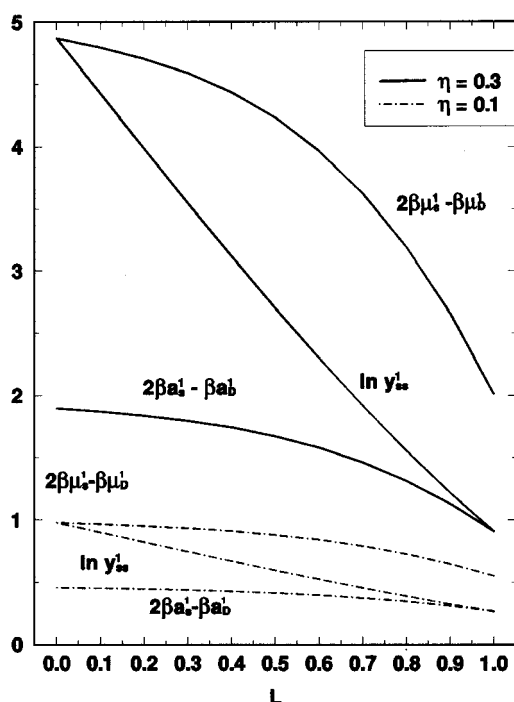
FIG. 4. Characterization of TPT1 for mixtures of hard spheres+symmetric dispheres. $\eta=0.1$ and 0.3. Similar behavior as in Fig. 2. Upper three solid curves are for $\eta=0.3$. The lower three dash–dot curves are for $\eta=0.1$. Note the confluence points at $L=1$.

FIG. 5. Interpolated Helmholtz free energy of pure symmetric dispheres at three $\eta=0.1$, 0.3, and 0.47. Circles: from Tildesley–Streett exact results. Solid lines: from Eq. (3.7) using 2.2 powers in bond length L. Dashed lines: from Eq. (3.6) using cubic powers in bond length L as prescribed by Phan–Kierlik–Rosinberg (Ref. 27).

cates that the prescription of TPT1 is valid at $L=1$ as stated by Wertheim, where the $\ln z$ function coincides with the cavity function (irrespective of the compositions x_D of the mixtures). $\ln z$ by construction is the Helmholtz free energy difference between those of the actual disphere fluid and a "hypothetical" reference dissociated fluid. By this way we are able to verify, through numerical calculations, the validity of the TPT1 prescription.

We want to examine whether the "difference property" also carries over to chemical potentials. We form the difference $2\beta\mu_S'^1 - \beta\mu_D'^1$ (where superscript 1 refers to pure monomers or pure dimers, i.e., they do not refer to the same mixture) and plot it in Fig. 3. We see that this quantity does not meet at the confluence point $L=1$. Therefore, the chemical potentials do not obey TPT1, while the Helmholtz free energies do.

At other packing fractions $\eta=0.1$ and 0.3, we observe the same behavior (Fig. 4). So this behavior is "universal," at least for the states examined. From these figures, we see that TPT1 works well for tangent dispheres ($L=1$). We also see why it fails for fused spheres (say at $L=0.5$). At $L=0.5$, the function $\ln z(L)$ is far removed from the cavity functions $\ln y(L)$ at any mole fractions. As Zhou and Stell noted, TPT1 is reasonable only for $L\geq0.8$. Figures 3 and 4 support this conclusion.

We examine further the curve $\ln z$. At $L=0$, $\ln z(L)$ approaches the pure monosphere Helmholtz free energy. For $L=1$, it approaches the cavity function of, say, pure monospheres $\ln y_{SS}^1(L=1)$. Both are well defined and accessible for hard spheres. We know these two limits. What is the behavior between these two limits? Phan, Kierlik and Rosin-
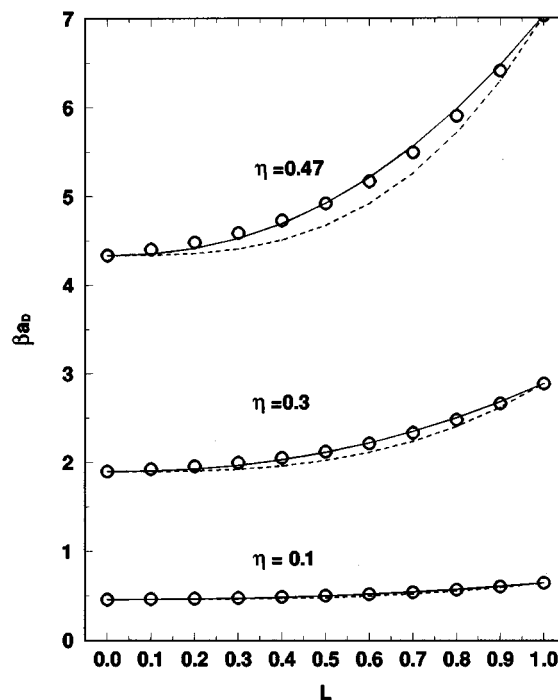
berg (PKR) have suggested an interpolation formula for reproducing the intermediate L behavior. They proposed a cubic power interpolation

$$\beta a_D'^1(L;\eta,x_D=1)\approx(1-L^3)\beta a_S'^1(\eta,x_S=1)+L^3\beta a_D'^1(L$$

$$=1;\eta,x_D=1). \qquad (3.6)$$

The important parameter is the packing fraction η that must be kept the same in the reference $\beta a_S'$ as in the tangent disphere $\beta a_D'(L=1)$. Since we can calculate all three quantities from the Boublík EOS, we can test the PKR interpolation formula (3.6). This is done in Fig. 5 for $\eta=0.47$. Comparison of the PKR results vs. the Boublík EOS results is presented at three packing fractions $\eta=0.1$, 0.3, and 0.47. It is seen that the cubic power interpolation is good at both ends $L=0$ and $=1$, but is poor near $L=0.5\sim0.6$. PKR underestimates the correct Helmholtz free energy considerably. At $\eta=0.3$, same poor agreement is seen. Only at low densities, PKR becomes reasonable. We also make a new attempt to fit the intermediate $\beta a_D'(L)$ behavior and found that a power of 2.2 will do well, i.e.,

$$\beta a_D'^1(L;\eta,x_D=1)\approx(1-L^{2.2})\beta a_S'^1(\eta;x_S=1)$$

$$+(L^{2.2})\beta a_D'^1(L=1;\eta,x_D=1). \qquad (3.7)$$

Figure 5 shows almost exact reproduction of the EOS results with this recipe. The number 2.2 was obtained empirically (PKR obtained the power 3 also by serendipity). However, Eq. (3.7) characterizes the TPT1 $\ln z(L)$ behavior accurately. At this juncture, it is not clear how to carry out an investigation from a purely theoretical perspective on the function
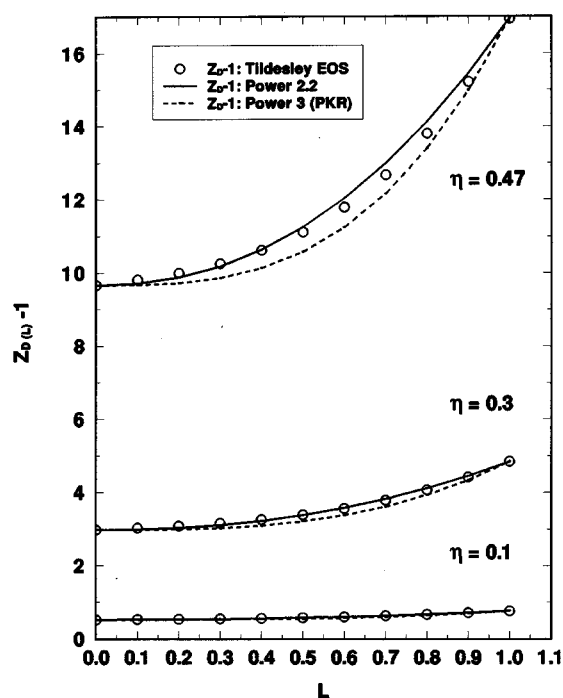
FIG. 6. Interpolated pressure of pure symmetric dispheres at three $\eta=0.1$, 0.3, and 0.47. Same notation as in Fig. 5. $Z=P/\rho kT$.

$\ln z$ for small L's. As pointed out earlier, $\ln z(L)$ of Eq. (3.5) involves terms that do not refer to the "same mixture." It is a relation between $\beta a_D'$ of the "real mixture" and $\beta a_S'$ of some "reference fluids," be it well chosen, at quite different compositions. This creates added complications vis-à-vis the second potential distribution theorem where all terms refer to the same mixture.

With a prescription for the Helmholtz free energy, we can calculate the pressures for symmetric pure hard dispheres via the thermodynamic relation: $\rho \partial \beta a_D'(L)/\partial \rho = \beta P'/\rho$ (prime indicates the configurational property). Figure 6 shows the comparison from the compressibility of the TS EOS at three packing fractions. Also shown are the PKR cubic power results. In general, PKR underpredicts the EOS values. The 2.2-power interpolation (3.7) works well, though some deviations near $L=0.7$ are noticeable. At least, we have a means for obtaining reasonable free energies and pressures for fused dispheres at any bond lengths. In Fig. 7, we compare the equations of state of Tildesley–Street and Boublík for symmetric dispheres. Very close agreement is obtained. Thus we can use either equation for characterization of symmetric dispheres. Next we shall look into the case of asymmetric hard dumbbells.

B. Asymmetric dispheres

We consider ternary mixtures of small spheres (S), big spheres (B), and heterodispheres (SB). The mole fractions of S and B are always kept the same $x_S=x_B$. The Boublík EOS is integrated to yield the chemical potentials $\beta\mu_S'$, $\beta\mu_B'$, $\beta\mu_{(SB)}'$ at five compositions $x_{(SB)}=0$, 0.3, 0.5, 0.8, and 1.0. The unlike cavity function $\ln y_{SB}(L;\eta,x_S,x_B,x_{(SB)})$ can be obtained again from the second PDT (3.1). These
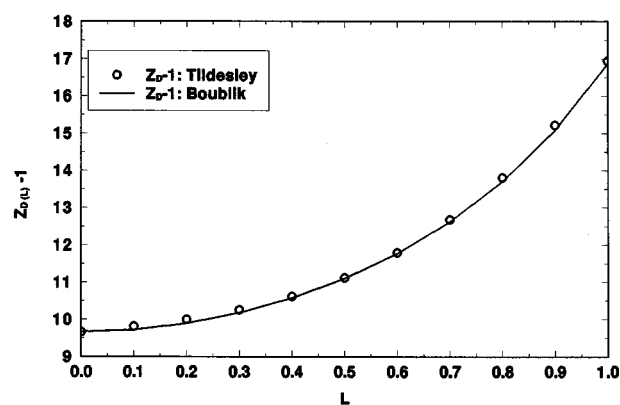

FIG. 7. Testing Boublík equation vs Tildesley–Streett equation for pure dumbbells. $\eta=0.47$.

values are presented in Fig. 8 for a constant packing fraction $\eta=0.408$. Since the big sphere (d_B) is 1.4925 times larger than the small sphere (d_S), the asymmetric tangent dispheres have a bond length of $L=l/d_S=1.246\,25$. At $L=1.246\,25$, again all cavity functions converge to a single *confluence point*. At $L\leq0.246\,25$, the small sphere of the dumbbell merges into its big neighbor. Then we have only a mixture of two types of monospheres (S and B) with $x_{(SB)}=0.0$. Because the final mole fractions were different, the chemical
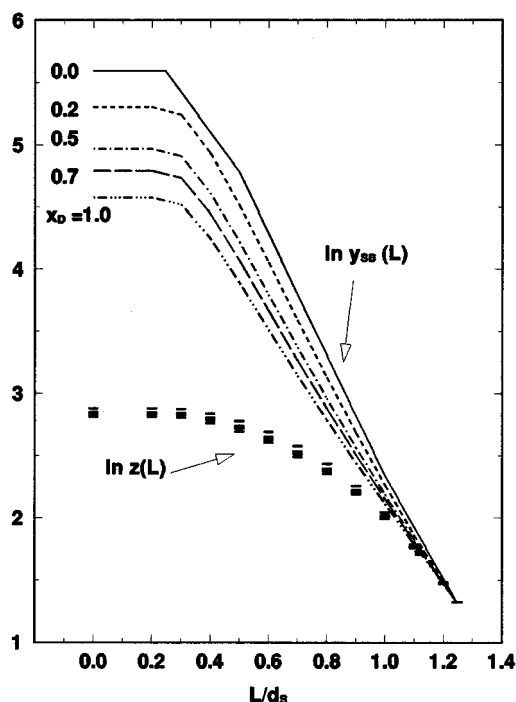

FIG. 8. Comparison of the cavity functions $\ln y_{SB}$ with the TPT1 function $\ln z$ (=Helmholtz free energy differences) for ternary mixtures of small spheres (S)+big spheres (B)+asymmetric dispheres (D) at mole fractions $x_D=0$, 0.2, 0.5, 0.7, and 1. Packing fraction $\eta=0.408$. Lines: $\ln y_{SB}$, the unlike cavity functions at five mole fractions. Five rows from top down: $x_D=0$, 0.2, 0.5, 0.7, and 1. Horizontal dashes: the TPT1 function $\ln z$ at four compositions, from top down $x_D=0.2$, 0.5, 0.7, and 1. These four isopleths are close to one another, but with visible differences. At $l=1.246\,25\,d_S$ (i.e., tangent disphere), all curves $\ln y$ and $\ln z$ meet at one point, the *confluence* point.

potentials of inserting a small sphere into such a bimono-meric fluid are nonetheless different from the original equimolar mixture. For example initially at $x_S = 0.25 = x_B$, and $x_{(SB)} = 0.5$, in the limit $L \rightarrow 0$, we have a mixture equivalent to $x_S = 0.25$, and $x_B = 0.75$. On the other hand, if initially $x_S = 0.3 = x_B$, and $x_{(SB)} = 0.4$, final fusion gives a mixture of $x_S = 0.3$, and $x_B = 0.7$. The final mixtures are different in mole fractions. In the same figure, we plot the TPT1 function $\ln z$

$$x_{(SB)} \ln z_{SB}(L; \eta, \hat{N}_S$$

$$= [x_S + x_{(SB)}] / [x_S + x_B + 2x_{(SB)}], \hat{N}_B$$

$$= [x_B + x_{(SB)}] / [x_S + x_B + 2x_{(SB)}])$$

$$= (1 + x_{(SB)}) \beta a'_{REF}(\eta) - \beta a'_{MIX}(L; \eta, x_S, x_B, x_{(SB)}),$$

$$(3.8)$$

where the reference fluid is an equimolar binary mixture of two types of monospheres S and B, $x_S = x_B$. It results from the total dissociation of all dimers in the real mixture. In practice, in order to keep η constant, the absolute numbers of reference monospheres have to be reduced in proportion (normalized, i.e., to $\hat{N}_S$ and $\hat{N}_B$) while maintaining the equal molar ratio of each species.

We observe from Fig. 8 that the TPT1 functions $\ln z(L)$ for the four compositions $x_{(SB)} = 0.2, 0.5, 0.7, 1.0$ collapse almost into a single curve (although some differences remain). This $\ln z$ is different from any of the $\ln y_{SB}$ curves (indication of failure of the TPT1 theory!) However, at a bond length equal to tangency $L = 1.246\ 25$, all four curves converge again at a *confluence point*. This figure says that the TPT1 theory is again valid at the tangent disphere limit (where $L = 1.246\ 25$). All the unlike cavity functions $\ln y_{SB}$ from PDT2 (at different compositions) also merge into this point. Therefore it is possible to use any one of the unlike cavity functions to obtain this confluence point, irrespective of their compositions. At the left end of the bond length spectrum $L \leqslant \delta = 0.246\ 25$, the heterodisphere fluid degenerates to monomeric big spheres (the small sphere is submerged into the big sphere). We already know the Helmholtz free energy of such hard spheres. Thus an interpolation can be formed to obtain $\ln z_{SB}(L)$ for intermediate values of L. Figure 9 shows the same type of interpolation by $L^{2.2}$ power as in Eq. (3.7) for $\beta a_{(SB)}$.

$$\beta a'^1_{(SB)}(L; \eta, x_{(SB)} = 1)$$

$$= (1 - (L - \delta)^{2.2}) \beta a'_{REF}(\eta, x_{(SB)} = 0)$$

$$+ ((L - \delta)^{2.2}) \beta a'^1_{(SB)}(L$$

$$= \text{tangency}; \eta, x_{(SB)} = 1)$$

$$\text{for } L \geqslant \delta,$$

$$(3.9)$$

where $\beta a'_{REF}$ is the reference equimolar binary monomer (small spheres+big spheres) mixture alluded above; $\beta a'_{(SB)}$ ($L = tangency$) is the Helmholtz free energy of tangent heterodispheres, all at same $\eta \cdot \delta = 0.5(d_B - d_S)$ is the submergence bond length (below which the small sphere is "devoured" by the big sphere). The Boublík $\beta a'_{(SB)}$ is well reproduced by the 2.2 power interpolation, while the cubic
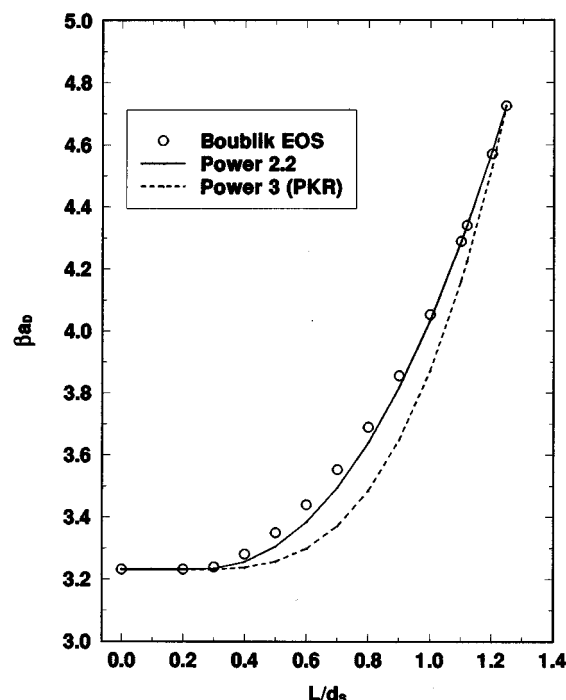

FIG. 9. Interpolated Helmholtz free energy of pure asymmetric dispheres at $\eta = 0.408$. Aspect ratio $d_B/d_S = 1.4925$. Circles: from Boublík exact results. Solid lines: from Eq. (3.9) using 2.2 powers in bond length L. Dotted lines: from the prescription of Phan–Kierlik–Rosinberg (Ref. 27) (PKR).

power interpolation of PKR underestimates the fused disphere values at intermediate L. Thus the same interpolation power 2.2 is shown to work for both asymmetric and symmetric dispheres.

Figure 10 examines the behavior of the three chemical potentials in the ternary mixtures according to the second PDT. Five mole fractions are displayed: $x_{(SB)} = 0$, 0.2, 0.5, 0.7, and 1.0. The important lesson to be drawn is that at the point of tangency ($L = 1.246\ 25$), all chemical potentials remain different. The mixtures can "feel" the difference during dimer insertion, even though the dimer is composed of two tangent spheres! However, in terms of cavity functions from Eq. (3.1), these effects are canceled out. One has a *unique* confluence point.

We obtain the pressures for fused heterodispheres at any L from the Helmholtz free energy Eq. (3.9) by density differentiation. The results are shown in Fig. 11 at $\eta = 0.408$. Excellent agreement with the Boublík EOS is obtained. PKR's cubic interpolation is also shown, with deficiencies in mid-ranges of L. There were simulation data for asymmetric dumbbells for η ranging 0.209 to 0.408, aspect ratios from 1.19 to 2.0, and bond lengths from 0.5 to 1.4925. The results are displayed in Fig. 12 with L as the x axis, η as the y axis, and $\beta P / \rho - 1$ as the z axis. We have shown the Boublík-calculated pressures (squares) together with the MC data (open circles). Boublík EOS is seen to perform outstandingly for heterodispheres at these conditions. The 2.2-power interpolation (filled circles) follows the MC data extremely well. The PKR cubic interpolation is generally below the MC data.
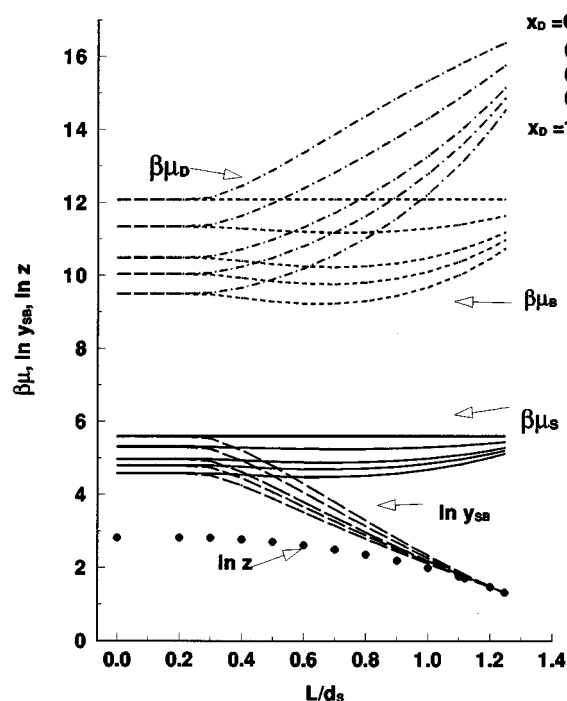
FIG. 10. Chemical potentials of ternary mixtures of asymmetric dispheres (D)+small (S) and big (B) monospheres. η=0.408. Dash–dot lines: dimer $\beta\mu'_D$ at five mole fractions x_D=0, 0.2, 0.5, 0.7, and 1 from top down. Dashed lines: big sphere $\beta\mu'_B$ at five mole fractions of x_D=0, 0.2, 0.5, 0.7, and 1 from top down. Solid lines: small sphere $\beta\mu'_S$ at five mole fractions of x_D, same order. Long dashed lines: $\ln y_{SB}$ from the potential distribution (3.1) at five mole fractions of x_D, same order. Circles: $\ln z_{SB}$ from the TPT1 Eq. (3.8) at x_D=1. We note that the three chemical potentials are all different at L=1.246 25 the tangent disphere limit. But a convergence point exists for all curves $\ln y$ and $\ln z$ at L=1.246 25.

FIG. 11. Interpolated pressure of pure asymmetric dispheres at η=0.408. Aspect ratio d_B/d_S=1.4925. Circles: from Boublík exact results. Solid lines: from Eq. (3.9) using 2.2 powers in bond length L. Dashed lines: from the prescription of Phan–Kierlik–Rosinberg (Ref. 27) (PKR).

IV. DISCUSSION

At this juncture, we make contact with previous works on the use of cavity functions. The first three papers of Zhou–Stell, especially number III,[36] have given a highly il-luminating use of cavity functions in the chemical equilibria of associating molecules and, in the limit, bonded chains. Since this work is partially inspired by these papers, a more detailed discussion is in order. Zhou–Stell have examined the *zeroth-order approximation* to the cavity functions based on an equal density reference monomer fluid. In this work, we examine a different behavior where the reference fluid is at the same packing fractions instead of at equal number densities. Zhou–Stell proposed a reacting mixture of *reactants A* and *B* with *product* (AB) at chemical equilibrium

$$A + \quad B \rightarrow \quad AB,$$
$$\rho_a \quad \rho_b \quad \rho_{(ab)}. \tag{4.1}$$

Thus the zero free energy change (equilibrium) requires that

$$\mu_a + \mu_b = \mu_{(ab)}. \tag{4.2}$$

The reaction was carried out from initially, say, an equimolar mixture of A and B with number densities $\rho_0 = \rho_a^0 = \rho_b^0$. The fractional conversion (or yield) α is the fraction of reactant A consumed
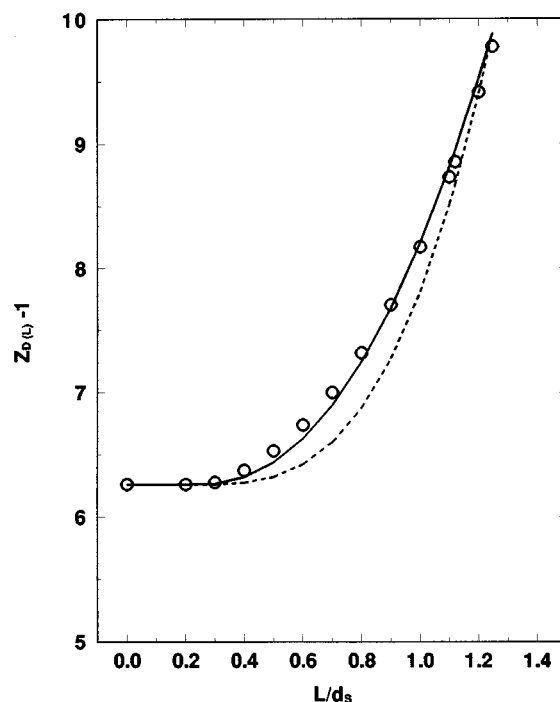
$$\alpha \equiv \frac{\rho_0 - \rho_a}{\rho_0} \tag{4.3}$$

or

$$\rho_a = \rho_0(1 - \alpha).$$

When α=0, we have the initial mixture of monomers $A + B$ (with $x_{(ab)}$=0). As $\alpha \rightarrow 1$, we have complete association: (with $x_{(ab)}$=1), where only (AB) dimers are present. Zhou and Stell showed that the chemical equilibrium constant K is related to the cavity function via Eq. (4.2)

$$\ln \frac{K}{K_0} = \ln y_{ab}(L) = \beta\mu'_a + \beta\mu'_b - \beta\mu'_{(ab)}(L) \tag{4.4}$$

for the product dimers of bond length L. They determined the behavior of $\ln K/K_0$ or $\ln y_{ab}(L)$ as a function of mono-mer density ρ_0 and bond length L. Interestingly, at bond length equal to the tangency value $l=0.5*(d_a+d_b)$, the cavity function $\ln y_{ab}(L=tangency)$ is identical to the zeroth-order approximation $\ln y_{ab}^0$

$$\ln y_{ab}(L=\text{tangency}; \eta, x_a, x_b, x_{(ab)} \neq 0)$$
$$= \ln y_{ab}^0(L=\text{tangency}; \eta_0, x_a^0, x_b^0, x_{(ab)}=0). \tag{4.5}$$

The zeroth-order approximation refers to a mixture where the dimer species AB is totally dissociated, and only monomers A and B are present (with the same numbers of monomers as the original mixture: $\rho_a^0 + \rho_b^0$, i.e., constant number density), very much in the spirit of Wertheim's TPT1. Here, the equal-ity (4.5) refers to the confluence point we have discussed above. Namely, $\ln y_{SB}(L; \eta, \mathbf{x})$ of mixtures of all composi-
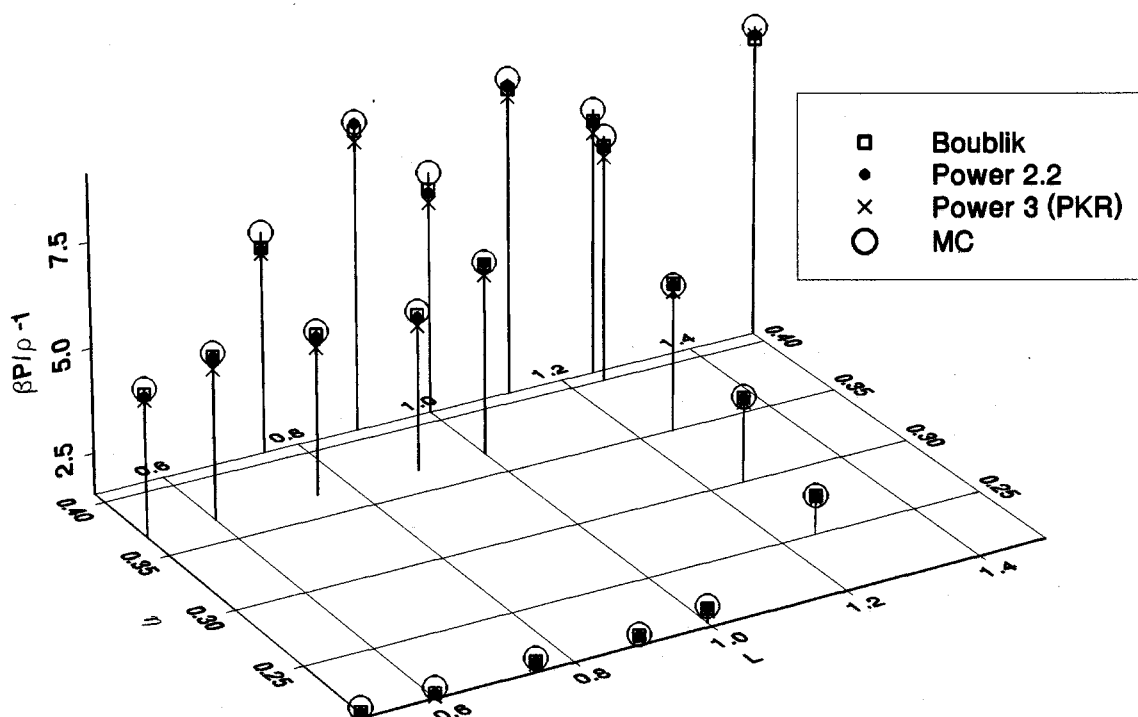
FIG. 12. Comparison with MC results for pressures of pure asymmetric dispheres at $\eta=0.209$ to 0.408, aspect ratios=1.19 to 2.0, and bond lengths $l/d_S=0.5$ to 1.5. Open circles=MC results. Squares=Boublík equation. Filled circles=from the 2.2 power interpolation, Eq. (3.9). XXX=from the cubic power interpolation of Phan *et al.* (Ref. 27). Conditions are given in Sec. III B.

tions will meet at L=tangency value. (Their figs. 2 and 6 of III showed this behavior at all densities.) However, when $L<$tangency, the zeroth-order cavity function $\ln y_{ab}^0$ yielded progressively poorer results. We need to examine the packing fractions η in Zhou–Stell. At a given α value, $0\leq\alpha\leq1$, we have the total packing fraction of the mixture $A+B+AB$

$$\eta(\alpha;L)=\rho_a\frac{\pi}{6}d_a^3+\rho_b\frac{\pi}{6}d_b^3+\rho_{(ab)}V_D(L)$$

$$=\rho_0\left[(1-\alpha)\frac{\pi}{6}(d_a^3+d_b^3)+\alpha V_D(L)\right]. \qquad (4.6)$$

Therefore, the packing fractions in Zhou–Stell were not constant, depending on the fractional conversion α. At L=tangency, however, V_D the dimer volume is equal to the sum of the volumes of the two constituent spheres. Then the packing fraction is the same as η_0 of the reference monomeric fluid (where both the total number density σ_Γ and the packing fraction η in the real mixture are equal to those of the *dissociated* mixture). Thus the TPT1 theory claims validity there.

At the other limit when $L\to0$, the dimer volume reduces to that of a big sphere. Zhou–Stell's η becomes

$$\eta(\alpha,L=0)=\rho_0\left[(1-\alpha)\frac{\pi}{6}d_a^3+\frac{\pi}{6}d_b^3\right]. \qquad (4.7)$$

This is not quite the packing fraction of the reference monomeric fluid [which still has $\sim2\rho_0$ as density, see Eq. (4.6) at $\alpha=0$]. Here, we have exposed some ambiguities in imple-

menting Wertheim's TPT1. In Wertheim[37] (1987), he set the reference fluid density $\rho_R(\bar1)=\sigma_\Gamma(\bar1)$ the total density (sum for monomers, bonded mers at the glue spots A, and B, etc.) In the tangent sphere limit, this prescription is fine, since the packing fraction is preserved. However, for highly eclipsed dispheres, $L\to0$, the packing fraction in the real mixture is drastically reduced, as shown by Eq. (4.6), sometimes to half the reference fluid value [Eq. (4.7)]. It is not likely that such a high density reference fluid will be able to represent the real fluid properties. Another anomaly is when the fused dispheres are already at a high packing fraction, say 0.47, the reference fluid of totally dissociated species, according to $\rho_R=\sigma_\Gamma$, will give an $\eta\approx0.94$, beyond the close packing limit! Phan, Kierlik, and Rosinberg[27] suggested maintaining a constant packing fraction during fusion, since hard core fluid properties are most sensitive to η. The PKR specification recovers the TPT1 choice at $L=1$, and behaves reasonably at $L\leq1$. We have adopted the PKR prescription throughout this work. In order to keep η constant, the number densities of the species involved will have to change as $L\to0$, but at fixed molar ratios with respect to one another.

In Zhou–Stell, the packing fraction η_0 of the reference fluid was much larger than η for the real fluid when $L=0$. Thus Fig. 6 of III[36] shows quite different curves between "exact" $\ln y$ and the zeroth-order $\ln y^0$, with the TPT1 theory overestimating $\ln y$, as expected.

In the present study, $L\to0$ gives another convergence point for the cavity functions, simply due to the fact that the same η is maintained in all mixtures. $\ln y_{SS}$ for pure dis-

pheres (*upon degenerating into single spheres*) is now identical to $\ln y_{SS}$ of the monospheres at the same η. We note that the variation of α in Zhou–Stell was equivalent to having different compositions in the ternary mixture of $A+B+AB$. However, by varying α, Zhou–Stell also changed η. For them, the TPT1 reference fluid was not at the same η as the real fluid. There was no convergence point at $L=0$ for Zhou–Stell. We point out this important difference here: this work examines constant η behavior, while Zhou–Stell examined the constant number density case. We have studied a different cross section of the behavior of $\ln y$. Next, we pursue a thermodynamic interpretation of Wertheim's TPT1.

Thermodynamic expressions. We derive some thermodynamic consequences of TPT1. Since the second potential distribution theorem gives the cavity distribution function in terms of purely thermodynamic quantities, we can derive the following thermodynamic relations. The density derivative of the cavity function is

$$\rho_S \frac{\partial \ln y_{SS}^1(L)}{\partial \rho_S} = 2\rho_S \frac{\partial \beta \mu_a'^1}{\partial \rho_S} - \rho_S \frac{\partial \beta \mu_D'^0(L)}{\partial \rho_S}. \quad (4.8)$$

This formula is of interest by itself. We obtain the density variations of the cavity function from purely thermodynamic considerations (with introduction of a dimer chemical potential at infinite dilution). A knowledge of the Henry's law constant will also give this information. On the other hand as L approaches tangency, the TPT1 gives the pressure as

$$\frac{\beta P_D'^1(L=1)}{\rho_D} = 2 \frac{\beta P_S'^1}{\rho_S} - \rho_S \frac{\partial \ln y_{SS}^1(L=1)}{\partial \rho_S}. \quad (4.9)$$

We shall treat from here on only tangent dispheres (L =tangency value). Substituting Eq. (4.8) into Eq. (4.9), and applying the Gibbs–Duhem relation, we can write the derivatives in terms of isothermal compressibilities

$$\frac{\beta P_D'^1}{\rho_D} = 2 \frac{\beta P_S'^1}{\rho_S} - 2 \frac{\partial \beta P_S'^1}{\partial \rho_S} + \rho_S \frac{\partial \beta \mu_D'^0}{\partial \rho_S}. \quad (4.10)$$

Equation (4.10) says that the pressure of pure dispheres is given (according to TPT1) by twice the pressure of monospheres (at same η) after subtracting the bonding terms, which include a density derivative of the infinite dilute chemical potential of a disphere in the reference fluid of monospheres. From Kirkwood–Buff fluctuation theory,[31] this derivative can be characterized as a direct correlation function integral

$$\frac{\partial \beta \mu_D^0}{\partial \rho_S} = -\lim_{\rho_D \to 0} \int d2 \, C_{SD}(2), \quad (4.11)$$

where $C_{SD}(2)$ is the direct correlation function between a monomer and a dimer. Using again the Gibbs–Duhem relation, we obtain

$$\rho_S \frac{\partial \beta \mu_D^0}{\partial \rho_S} = \lim_{\rho_D \to 0} \frac{\partial \beta P}{\partial \rho_D} - 1. \quad (4.12)$$

Thus we should be able to obtain the tangent disphere pressure from purely thermodynamic considerations. Equally, we can obtain the cavity function derivative from thermody-

namic relations. Relation (4.8) supplements the zero-separation theorems that already exist for the cavity functions.

V. CONCLUSIONS

We have presented here three potential distribution theorems in alternative forms that relate the monomer, dimer, and trimer chemical potentials to not only the cavity distribution functions $\ln y^{(2)}$, and $\ln y^{(3)}$, but also to the singlet direct correlation function $C_a^{(1)}(\mathbf{r}_N; w)$. Some new formulas are derived (e.g., the alternative PDT3). With an accurate equation of state (e.g., the Boublík EOS) for calculating the chemical potentials of monomers and dimers, we have determined the cavity functions in ternary mixtures via the second potential theorem (3.1).

We ascertained the behavior of the cavity functions for different mixtures of hard dispheres and monospheres at bond lengths from $L=0$ to the length of tangency $[l=0.5(d_B+d_S)]$. Two interesting observations are obtained: (i) all cavity functions (at different molar compositions of monomers and dimers) converge to a single point, the *confluence point* when the bond length reaches the tangency value. This is so for both symmetric and asymmetric dispheres. (ii) The Wertheim TPT1 theory for the Helmholtz free energies is valid at bond length=tangency value. However, for L less than 80%~90% the tangency length, the Wertheim $\ln z(L)$ function differs appreciably from the cavity functions $\ln y$.

In order to have an accurate formula for the Helmholtz free energy of fused dumbbells, we fitted à la Phan–Kierlik–Rosinberg the fused disphere Helmholtz free energy and pressure to a formula containing 2.2 powers of the bond length L. This interpolation formula works well for both symmetric and asymmetric dispheres at any L (within the accuracy of the Boublík equation of state). By using the recipes of Phan–Kierlik–Rosinberg, further interpolations can be made to extend to higher length chains. We cite a fused triatomic, as an example. This fused heterotrisphere with three segments a, b, and c shall be denoted by us as $(a\char`^b\char`^c)$. ($\char`^$ denotes fusion between neighbors.) On the other hand, a *tangent* heterotrisphere is represented as $(a,b,c)$. (Comma "," denotes tangent bond between neighbors.) A two-level procedure was used by PKR.[27] On the first level, the Helmholtz free energy (or compressibility) of $(a\char`^b\char`^c)$ can be obtained as interpolation between two other quite different heteropolyspheres, i.e., $(a,b\char`^c)$ and $(b\char`^c)$. This interpolation follows Eq. (3.9), because the $a$ sphere can be fused, starting from tangency to a desired bond length $L_{ab}$ from the center $b$ sphere, provided properties of $(a,b\char`^c)$ and $(b\char`^c)$ are already known. Next on the second level: (1) $(a,b\char`^c)$ is obtained from interpolating two tangent heteropolyspheres: (a,b) and (a,b,c); while (2) $(b\char`^c)$ is obtained from interpolating $(b)$ and $(b,c)$. On the lowest (second) level, all polyspheres are tangent. Equation (3.9) can again be used to good effects. By successive fusions, we can build up to the fused trisphere $(a\char`^b\char`^c)$. We have illustrated by trimers the procedure for obtaining properties of higher fused heterochains using the simple 2.2 power interpolation formula (3.9). We caution that for a more precise

treatment of long-chain heteropolyspheres, the correct cavity function for each pair of neighbors should be used, as in the SAFT-dimer theory of Ghonasgi and Chapman.[38]

A general theoretical framework is provided for research into soft potential models. Formulas which are purely thermodynamic in nature have been derived from TPT1 and for the derivatives of the cavity functions. Alkane molecules have fusion in the range of $L=0.3\sim0.5$. Copolymers have segments with different sizes. Proper extensions of the present approach hold promise for treating these important classes of heterochains. Chemical association can also be treated within the present theory. Implications to the general theory on molecular correlation functions will be explored.

ACKNOWLEDGMENTS

[1] M. S. Wertheim, J. Stat. Phys. **35**, 19 (1984); **35**, 35 (1984); **42**, 459 (1986); **42**, 477 (1986); J. Chem. Phys. **85**, 2929 (1986); **87**, 7323 (1987); **88**, 1145 (1988).

[2] E. Kierlik and M. L. Rosinberg, J. Stat. Phys. **68**, 1037 (1992); E. Kierlik and M. L. Rosinberg, Phy. Rev. A **44**, 5025 (1991); E. Kierlik and M. L. Rosinberg, J. Chem. Phys. **97**, 9222 (1991); E. Kierlik and M. L. Rosinberg, *ibid*. **99**, 3950 (1993); **100**, 1716 (1994).

[3] R. Dickman and C. K. Hall, J. Chem. Phys. **85**, 4108 (1986); K. G.. Honnell and C. K. Hall, *ibid*. **90**, 1841 (1989).

[4] Y. C. Chiew, Mol. Phys. **70**, 129 (1990); J. Chem. Phys. **93**, 5067 (1990); Mol. Phys. **73**, 359 (1991).

[5] J. G. Curro and K. S. Schweizer, J. Chem. Phys. **87**, 1842 (1987); K. S. Schweizer and J. G. Curro, Macromolecules **20**, 3070 (1987). K. S. Schweizer and J. G. Curro, J. Chem. Phys. **89**, 3342 (1988).

[6] W. G. Chapman, K. E. Gubbins, C. G. Joslin, and C. G. Gray, Fluid Phase Equil. **29**, 337 (1986); W. G. Chapman, and K. E. Gubbins, Pure Appl. Chem. **59**, 53 (1987); C. G. Joslin, C. G. Gray, W. G. Chapman, and K. E. Gubbins, Mol. Phys. **62**, 843 (1987); W. G. Chapman, G. Jackson, and K. E. Gubbins, *ibid*. **65**, 1057 (1988); W. G. Chapman, K. E. Gubbins, G. Jackson, and M. Radosz, Fluid Phase Equil. **52**, 31 (1989); W. G. Chapman, K. E. Gubbins, G. Jackson, and M. Radosz, I&EC Res. **29**, 31 (1990).

[7] G. Jackson, W. G. Chapman, and K. E. Gubbins, Mol. Phys. **65**, 1 (1988); G. Jackson and K. E. Gubbins, Pure Appl. Chem. **61**, 1021 (1989); G. Jackson, Mol. Phys. **72**, 1365 (1991).

[8] G. Jackson, Mol. Phys. **72**, 1365 (1991); D. G. Green and G. Jackson, J. Chem. Soc. Faraday Trans. **88**, 1395 (1992); J. Chem. Phys. **101**, 3190 (1994); S. H. Huang and M. Radosz, Ind. Eng. Chem. Res. **29**, 2284 (1990); S. H. Huang and M. Radosz, Ind. Eng. Chem. Res. **30**, 1994 (1991).

[9] J. K. Johnson, E. A. Mueller, and K. E. Gubbins, J. Chem. Phys. **98**, 6413 (1994).

[10] W. G. Chapman, J. Chem. Phys. **93**, 4299 (1990); J. K. Johnson and K. E.

Gubbins, Mol. Phys. **77**, 1033 (1992); D. Ghonasgi and W. G. Chapman, *ibid*. **79**, 291 (1993); D. Ghonasgi and W. G. Chapman, *ibid*. **80**, 161 (1993); D. Ghonasgi and W. G. Chapman, AIChE J. **40**, 878 (1994); J. Chem. Phys. **100**, 6633 (1994); D. Ghonasgi, V. Perez, and W. G. Chapman, *ibid*. **101**, 6880 (1994); D. Ghonasgi and W. G. Chapman, Mol. Phys. **83**, 145 (1994).

[11] R. P. Sear and G. Jackson, Mol. Phys. **82**, 473 (1994). R. P. Sear and G. Jackson, *ibid*. **83**, 961 (1994); D. Ghonasgi and W. G. Chapman, AIChE J. **40**, 878 (1994).

[12] J. M. Walsh and K. E. Gubbins, J. Phys. Chem. **94**, 5115 (1990). M. D. Amos and G. Jackson, J. Chem. Phys. **96**, 4604 (1992).

[13] H. Reiss, H. L. Frisch, and J. L. Lebowitz, J. Chem. Phys. **31**, 369 (1959); R. M. Gibbons, Mol. Phys. **17**, 81 (1969).

[14] E. Meeron and A. J. F. Siegert, J. Chem. Phys. **48**, 3139 (1968); E. W. Grundke and D. Henderson, Mol. Phys. **24**, 269 (1972).

[15] B. Widom, J. Chem. Phys. **39**, 2808 (1963); B. Widom, J. Stat. Phys. **19**, 563 (1978).

[16] See, for example, in L. L. Lee, *Molecular Thermodynamics of Nonideal Fluids* (Butterworths, Boston, 1988).

[17] L. Verlet, Mol. Phys. **41**, 183 (1980).

[18] K. S. Shing and K. E. Gubbins, Mol. Phys. **43**, 717 (1981); K. S. Shing and K. E. Gubbins, *ibid*. **46**, 1109 (1982); S. Romano and K. Singer, *ibid*. **37**, 1765 (1979); J. G. Powles, *ibid*. **41**, 715 (1980).

[19] L. L. Lee and K. S. Shing, *Potential Distribution of Anisotropic Molecules* (West Coast Statistical Mechanics Conference, 1989).

[20] S. K. Kumar, I. Szleifer, and A. Z. Panagiotopoulos, Phys. Rev. Lett. **66**, 2935 (1991); edited Computer Simulations of Polymers, edited by E. A. Colbourn (Longman, Harlow, 1992).

[21] T. Boublík, Mol. Phys. **59**, 775 (1986).

[22] L. L. Lee, J. Chin. Inst. Chem. Eng. **19**, 337 (1988).

[23] G. Stell and Y. Zhou, J. Chem. Phys. **91**, 3618 (1989); K. Olaussen and G. Stell, J. Stat. Phys. **62**, 221 (1991); Y. Zhou and G. Stell, J. Chem. Phys. **96**, 1504 (1992); Y. Zhou and G. Stell, *ibid*. **96**, 1507 (1992); G. Stell and Y. Zhou, Fluid Phase Equil. **79**, 1 (1992).

[24] L. L. Lee, J. Chem. Phys. **97**, 8606 (1992).

[25] D. J. Tildesley and W. B. Streett, Mol. Phys. **41**, 85 (1980).

[26] T. Boublík, J. Chem. Phys. **63**, 4084 (1975); I. Nezbeda and T. Boublík, Czech. J. Phys. B **27**, 1073 (1977); T. Boublík, Mol. Phys. **44**, 1369 (1981); **59**, 371 (1986).

[27] S. Phan, E. Kierlik, and M. L. Rosinberg, J. Chem. Phys. **101**, 7997 (1994).

[28] R. J. Speedy and H. Reiss, Mol. Phys. **72**, 999 (1991).

[29] J. G. Kirkwood and F. P. Buff, J. Chem. Phys. **19**, 774 (1951). See, for example, a review by L. L. Lee, P. G. Debenedetti, and H. D. Cochran, in *Supercritical Fluid Technology*, edited by T. J. Bruno and J. F. Ely (CRC, Boca Raton, 1991).

[30] B. Widom, J. Chem. Phys. **39**, 2808 (1963).

[31] L. L. Lee and K. S. Shing, J. Chem. Phys. **91**, 477 (1989).

[32] S. Labik, A. Malijevsky, and W. R. Smith, Mol. Phys. **83**, 983 (1994); **83**, 1223 (1994).

[33] J. Yvon, *La Théorie Statistique des Fluides et l' Equation d' Etat* (Actualités Scientifiques et Industrielles, No. 203, Paris, 1935).

[34] See, for example, E. Lomba and L. L. Lee, *Proceedings of the 12th Symposium on Thermophysical Properties* (Boulder, Colorado, 1994).

[35] E. Byckling, Physica **27**, 1030 (1961); R. J. Speedy and H. Reiss, Mol. Phys. **72**, 999 (1991); R. K. Bowles and R. J. Speedy, *ibid*. **83**, 113 (1994).

[36] Y. Zhou and G. Stell, J. Chem. Phys. **96**, 1507 (1992).

[37] M. S. Wertheim, J. Chem. Phys. **87**, 7323 (1987).

[38] D. Ghonasgi and W. G. Chapman, J. Chem. Phys. **100**, 6633 (1994).